

Asymptotic Scaling Laws for Imploding Thin Fluid Shells

M. M. Basko* and J. Meyer-ter-Vehn

Max-Planck-Institut für Quantenoptik, D-85748 Garching, Germany

(Received 5 February 2002; published 30 May 2002)

Scaling laws governing implosions of thin shells in converging flows are established by analyzing the implosion trajectories in the (A, M) parametric plane, where A is the in-flight aspect ratio, and M is the implosion Mach number. Three asymptotic branches, corresponding to three implosion phases, are identified for each trajectory in the limit of $A, M \gg 1$. It is shown that there exists a critical value $\gamma_{cr} = 1 + 2/\nu$ ($\nu = 1, 2$ for, respectively, cylindrical and spherical flows) of the adiabatic index γ , which separates two qualitatively different patterns of the density buildup in the last phase of implosion. The scaling of the stagnation density ρ_s and pressure P_s with the peak value M_0 of the Mach number is obtained.

DOI: 10.1103/PhysRevLett.88.244502

PACS numbers: 47.40.-x, 52.57.Bc

Compression of matter to very high densities is an interesting fundamental problem in itself, and a crucial issue in certain applications as, for example, inertial confinement fusion (ICF) [1]. In practical terms, it is usually a problem of reaching as high as possible matter density by applying a given limited external pressure $p \leq P_0$. When applied quasistatically, a given pressure P_0 can produce only a limited maximum density ρ_0 , which corresponds to a practical minimum of the specific entropy in the compressed sample.

The way to unlimited (at least in principle) compression of matter is opened by symmetrical implosions of thin fluid shells in a converging (cylindrical or spherical) geometry. So long as the hydrodynamic instabilities and drive asymmetries are kept under control, arbitrarily high matter densities (although for a brief instant only) can be reached behind the return shock after a sufficiently thin shell, accelerated by a fixed external pressure P_0 , converges to the center of symmetry. Here we address a pure problem of ideal one-dimensional (1D) hydrodynamics, namely, we establish how pressure and density (and the corresponding specific entropy) at stagnation scale with the shell in-flight aspect ratio A and its Mach number M in the asymptotic limit of $A, M \gg 1$. Knowing this scaling allows one to answer such questions as, for example, how much thinner a shell should be taken in order to achieve a desired enhancement in the degree of compression.

The reason why this basic problem has not been solved before lies in the difficulty of describing nonlinear converging flows and, in particular, of determining the entropy generated in the stagnating fluid behind the shock rebounding from the center. Kemp *et al.* [2] made use of a self-similar solution for a spherical shell imploding with a Mach number M_0 [3] and obtained an approximate scaling $P_s/P_0 \propto M_0^{3,0}$ ($\gamma = 5/3$) for an intermediate range of Mach numbers $2 \lesssim M_0 \lesssim 20$. However, it remained unclear what happens in the limit of $M_0 \rightarrow \infty$, and how this self-similar solution could be related to properties of the accelerating pressure pulse. Here we approach the problem from a different side, not requiring self-similarity but restricting ourselves to asymptotic values of $A, M \gg 1$.

Analytically derived scaling laws are validated by numerical simulations.

Once a specific implosion strategy is chosen and fixed, the entire multitude of all possible states of imploding shells may be considered as a five-parameter family of snapshot spatial profiles for the density $\rho(t, r)$, velocity $u(t, r)$, and pressure $p(t, r)$. We choose the peak density $D = D(t) = \max_r \rho(t, r) \equiv \rho(t, R)$, the corresponding pressure $P(t) = p(t, R)$, the implosion velocity $U(t) = -u(t, R)$, the shell radius $R(t)$, and its effective thickness

$$h = h(t) = \frac{1}{D} \int_0^\infty \rho(t, r) dr \quad (1)$$

to be such parameters.

Optimal implosion strategy for the highest degree of final compression, as described in detail in Ref. [4], is accomplished by (i) setting a cold shell in motion by a carefully tailored pressure pulse, which generates a minimum amount (if any) of entropy, followed by (ii) the phase of adiabatic acceleration to a maximum implosion velocity by the peak boundary pressure P_0 . Here we omit the first phase—which is absolutely insignificant for the scaling laws in question—and start with an isentropic density profile across a motionless shell,

$$\rho(0, r) = D_0 \left(\frac{r - r_0}{R_0 - r_0} \right)^{1/(\gamma-1)}, \quad (2)$$

which corresponds to a uniform acceleration of all fluid elements (a UA, i.e., uniformly accelerated, profile) by a fixed pressure P_0 at the outer boundary; γ is the adiabatic index. The interior of the shell at $0 < r < r_0$ is void. The initial effective shell thickness is $h_0 = (1 - \gamma^{-1})(R_0 - r_0)$. Under such drive conditions no shocks pass through the shell until the very moment of void closure, and the entropy parameter $\alpha \equiv P/\rho^\gamma = \alpha_0 = P_0/D_0^\gamma$ remains constant in space and time.

From the five-dimensional parameters P, D, U, R , and h , which define the state of a shell in flight, only two dimensionless combinations can be constructed, namely,

the in-flight aspect ratio $A = R/h$, and the Mach number $M = U/C$. [To simplify the formulas, we define the Mach number with respect to the isothermal speed of sound $C = (P/D)^{1/2}$.] Hence, each implosion is represented by a trajectory in the (A, M) parametric plane. All possible implosions (within a fixed implosion strategy) are given by a one-parameter family of such trajectories. As a dimensionless parameter, identifying an individual implosion trajectory, either the initial aspect ratio $A_0 = R_0/h_0$ or the maximum Mach number M_0 [see Eq. (7) below] can be chosen. Clearly, such dimensionless quantities as the ratios between the stagnation and the initial pressures and densities are uniquely determined by the value of A_0 (or M_0)—in combination, of course, with the γ and ν values, where $\nu = 0, 1, 2$ corresponds, respectively, to planar, cylindrical, and spherical flows.

We base our analysis on the equations of mass balance,

$$m = DhR^\nu = D_0h_0R_0^\nu = \text{const}, \quad (3)$$

energy balance,

$$\frac{P_0(R_0^{\nu+1} - R^{\nu+1})}{\nu + 1} = \frac{1}{2} mU^2, \quad (4)$$

and a comparison between two relevant time scales

$$t_h = \frac{h}{C} \quad \text{and} \quad t_{im} = \frac{R}{U}, \quad (5)$$

where t_h is the time scale of hydrodynamic relaxation of the density (pressure) profile across the shell, and t_{im} is the implosion time. Equations (3) and (4) apply to thin ($A \gg 1$) shells in the limit of $M \gg 1$. For simplicity, we have omitted the unimportant geometrical factor 4π (2π) for spherical (cylindrical) shells.

Relation between the time scales t_h and t_{im} divides the (A, M) plane into two domains. In regions *A* and *B*, where the two initial phases of implosion occur (see Fig. 1), the ratio $t_h/t_{im} = M/A \ll 1$. This means that the density distribution across the shell relaxes to the equilibrium profile, corresponding to the adopted boundary condition, much faster than the effects of flow convergence

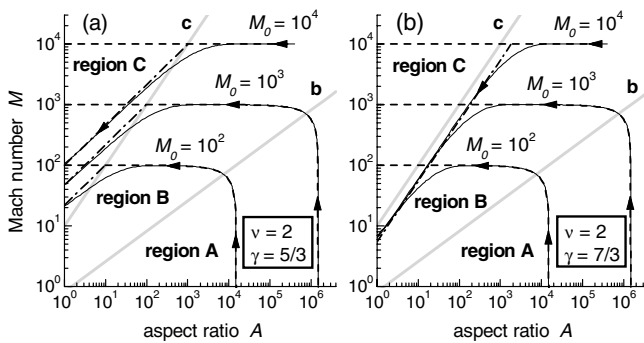


FIG. 1. Implosion trajectories for (a) $\gamma < \gamma_{cr}$ and (b) $\gamma > \gamma_{cr}$. Results of numerical simulations (thin solid) are compared with the asymptotic expression (6) for regions *A* and *B* (dashed), and Eq. (12) for region *C* (dash-dotted). Lines *b* and *c* separate three successive phases (*A*, *B*, and *C*) of implosion.

distort it. As a result, the density profile preserves the UA shape corresponding to the fixed boundary pressure P_0 , with $D = D_0$ being constant and the areal density varying as $\int \rho dr = D_0h \propto R^{-\nu}$. This condition, combined with Eqs. (3) and (4), leads to the following analytical expression for the implosion trajectories:

$$M = \left[\frac{2}{\nu + 1} (A_0 - A) \right]^{1/2} = \left(M_0^2 - \frac{2}{\nu + 1} A \right)^{1/2}. \quad (6)$$

Here we have introduced the maximum Mach number

$$M_0 = \left(\frac{2}{\nu + 1} A_0 \right)^{1/2}. \quad (7)$$

The divide line between the phase *A* of initial acceleration and the phase *B* of “relaxed” converging flow is given by

$$\text{line } b: \quad M = \left(\frac{2}{\nu + 1} A \right)^{1/2}. \quad (8)$$

Figure 1 demonstrates a perfect agreement between Eq. (6) and the results of numerical simulations in regions *A* and *B*. Simulations have been done with the 1D hydrodynamics code DEIRA [5], based on a Lagrangian scheme with a tensor artificial viscosity. The DEIRA code has been designed and extensively tested for simulating ICF fusion capsules. For the present problem, the code has been modified to treat a central void cavity. The initial state was assigned as an isentropic UA profile (2) at rest, and a fixed pressure $p = P_0$ was used as an outer boundary condition. A zero pressure before the void closure and a zero velocity after the void closure were used as a boundary condition at the inner shell edge. Typically, 150 mesh cells across the shell thickness were used.

Examination of the implosion dynamics in region *C*, where $t_h \gg t_{im}$, reveals that there exists a critical value of the adiabatic index,

$$\gamma_{cr} = 1 + \frac{2}{\nu}, \quad (9)$$

which separates two qualitatively different implosion patterns. For an imploding state in region *C*, the density buildup due to flow convergence occurs much faster than it can relax to the pertinent boundary condition. Then, one can tentatively assume that the shell thickness $h(t)$ becomes asymptotically “frozen” at a certain constant value h_1 as the shell radius $R \rightarrow 0$. Under this assumption the peak density increases as $D \propto R^{-\nu}$, and the large ratio

$$\frac{t_h}{t_{im}} = \frac{M}{A} \propto D^{(1-\gamma)/2} R^{-1} \propto R^{\nu(\gamma-1)/2-1} \quad (10)$$

becomes even larger as $R \rightarrow 0$ for $\gamma < \gamma_{cr}$ [the implosion velocity U saturates at its limiting value, given by Eq. (4) for $R \ll R_0$]. As a consequence, the assumption of a frozen shell thickness h becomes better and better justified, and the implosion trajectory, once in region *C*, tends to

penetrate deeper in this region, away from the divide line c where $t_h \approx t_{im}$, and approaches asymptotically the power law

$$M \propto C^{-1} \propto D^{(1-\gamma)/2} \propto A^{\nu(\gamma-1)/2}. \quad (11)$$

The latter is clearly illustrated in Fig. 1a with numerically calculated implosion trajectories.

For $\gamma > \gamma_{cr}$, on the opposite, the ratio t_h/t_{im} , once initially large, decreases with $R \rightarrow 0$, and an implosion trajectory, once in region C , is pushed out back to region B . The latter means that, for a fixed boundary pressure, implosion trajectories never actually cross to region C . Rather, having approached the divide line $M \propto A$ from region B , they turn away from the asymptotic law (6) and follow the line $M \propto A$, corresponding to $t_h \approx t_{im}$. The combined effect of the density growth due to flow convergence and the competing relaxation due to hydrodynamic expansion, both of which act on the same time scale $t_h \approx t_{im}$, results in that finally all the implosion trajectories with different M_0 develop the same asymptotic density profile and converge to a single (for given ν and $\gamma > \gamma_{cr}$) path (an attractor) in the (A, M) plane—as it is clearly seen in Fig. 1b.

The above considerations, combined with Eqs. (3) and (4), lead to the following asymptotic expressions for the implosion trajectories in phase C ,

$$M = \begin{cases} M_0^{1-\nu(\gamma-1)/2} (K_{c0}A)^{\nu(\gamma-1)/2}, & \gamma < \gamma_{cr}, \\ K_{c\gamma}A, & \gamma > \gamma_{cr}. \end{cases} \quad (12)$$

Here we have introduced two unknown coefficients, namely, K_{c0} , which defines the divide line,

$$\text{line } c: \quad M = K_{c0}A, \quad (13)$$

between regions B and C in the case of $\gamma < \gamma_{cr}$, and the slope $K_{c\gamma}$ of the limiting implosion path for $\gamma > \gamma_{cr}$. The dependence on M_0 in Eq. (12) for $\gamma < \gamma_{cr}$ is recovered by observing that lines (11) and (13) both cross the $M = M_0$ line at the same point. From numerical simulations we infer the value of $K_{c0} = 10.0 \pm 0.5$, which shows practically no dependence on ν and γ . The coefficient $K_{c\gamma}$ can be calculated analytically (the details are to be published elsewhere),

$$K_{c\gamma} = \frac{\gamma + 1}{\gamma - 1} \left\{ \frac{2\pi\gamma}{(\nu + 1)[\nu(\gamma - 1) - 2]} \right\}^{1/2} \times \frac{\Gamma(\frac{\gamma}{\gamma-1})}{\Gamma(\frac{1}{2} + \frac{\gamma}{\gamma-1})}, \quad (14)$$

where $\Gamma(x)$ is Euler's gamma function. The asymptotic law of density growth in phase C —the phase of compression by flow convergence—is given by

$$D \propto \begin{cases} R^{-\nu}, & \gamma < \gamma_{cr}, \\ R^{-2(\nu+1)/(\gamma+1)}, & \gamma > \gamma_{cr}. \end{cases} \quad (15)$$

Implosion of a shell ends when the central void closes and a return shock stops the infalling material. This occurs when the aspect ratio A falls below a certain value $A_1 \approx 1$ (which, in general, depends on ν and γ). Equation (12)

tells us that the amplitude of the return shock, determined by the corresponding Mach number,

$$M_1 \propto \begin{cases} M_0^{1-\nu(\gamma-1)/2}, & \gamma < \gamma_{cr}, \\ \text{const}, & \gamma > \gamma_{cr}, \end{cases} \quad (16)$$

becomes infinitely large in the limit of $M_0 \rightarrow \infty$ for $\gamma < \gamma_{cr}$, and approaches a finite value for $\gamma > \gamma_{cr}$. Hence, the return shock compresses the infalling matter by a limiting factor $(\gamma + 1)/(\gamma - 1)$ for $\gamma < \gamma_{cr}$, and by a smaller finite factor for $\gamma > \gamma_{cr}$. As a result, we obtain the following scaling law:

$$\frac{\rho_s}{\rho_0} \propto \left(\frac{M_0}{M_1} \right)^{2/(\gamma-1)} \propto \begin{cases} M_0^\nu, & \gamma < \gamma_{cr}, \\ M_0^{2/(\gamma-1)}, & \gamma > \gamma_{cr}, \end{cases} \quad (17)$$

for the ratio between the stagnation density ρ_s and the initial peak density $\rho_0 \equiv D_0$. Here ρ_s is some characteristic density at stagnation behind the return shock, representative of the bulk of the shell mass (because of a singularity occurring in the ideal hydrodynamics at $r = 0$ at void closure, the infinite peak density behind the return shock is of no practical interest).

The scaling of the stagnation pressure P_s is established by extending the energy equation (4),

$$\frac{P_s V_s}{\gamma - 1} = \frac{P_0 R_0^{\nu+1}}{\nu + 1} = \frac{1}{2} m \frac{P_0}{D_0} M_0^2, \quad (18)$$

to the stagnation state, for which we ignore the kinetic energy in comparison with the thermal one. Since the total volume V_s at stagnation scales as $V_s \propto m/\rho_s$, we arrive at

$$\frac{P_s}{P_0} \propto \frac{\rho_s}{\rho_0} M_0^2 \propto \begin{cases} M_0^{\nu+2}, & \gamma < \gamma_{cr}, \\ M_0^{2\gamma/(\gamma-1)}, & \gamma > \gamma_{cr}. \end{cases} \quad (19)$$

Equations (17) and (19) allow us to relate the values of the adiabat parameter $\alpha \equiv P/\rho^\gamma$ before and after the stagnation,

$$\frac{\alpha_s}{\alpha_0} \propto \left(\frac{\rho_s}{\rho_0} \right)^{1-\gamma} M_0^2 \propto \begin{cases} M_0^{2-\nu(\gamma-1)}, & \gamma < \gamma_{cr}, \\ \text{const}, & \gamma > \gamma_{cr}. \end{cases} \quad (20)$$

By using Eq. (7), one can rewrite Eqs. (17), (19), and (20) in terms of the initial in-flight aspect ratio A_0 .

Scaling laws (17), (19), and (20) are fully confirmed by our numerical 1D hydrodynamic simulations. The results for the α_s scaling are shown in Fig. 2. The agreement for the ρ_s/ρ_0 and P_s/P_0 ratios is equally good. For the case of $\nu = 2$, $\gamma = 5/3$, which is most relevant to ICF, we calculate

$$\alpha_s = (0.62 \pm 0.01) \alpha_0 M_0^{2/3}. \quad (21)$$

Because the specific entropy distribution behind the return shock is not uniform, the numerical coefficient in Eq. (21) depends on the choice of the reference point. In simulations, the values of ρ_s , P_s , and α_s were taken at the midpoint with respect to the mass coordinate of the shell. Remarkably, the asymptotic relationships (17), (19), and (20), valid in the limit of $M_0 \rightarrow \infty$, become already quite accurate for the values of M_0 as low as $M_0 \approx 10$.

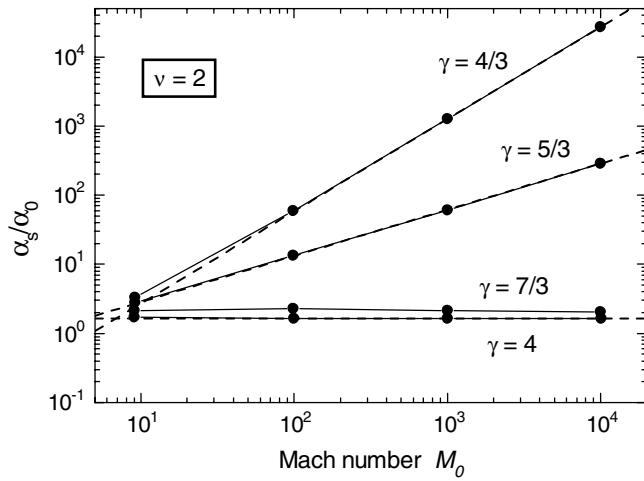


FIG. 2. Scaling of the stagnation adiabat parameter $\alpha_s = P_s/\rho_s^\gamma$ with the maximum Mach number M_0 . Numerical results (black dots) are compared with the asymptotic formula (20) (dashed lines).

The principal difference between our scaling and that of Ref. [2] is that the pressure scaling has been obtained in Ref. [2] as a power-law fit to the non-power-law dependence on M_0 calculated from the self-similar solution for an intermediate range of $2 \lesssim M_0 \lesssim 20$. Our scaling, on the contrary, may be considered as an exact analytic result for the limit of $M_0 \rightarrow \infty$. Quantitatively, the difference at $\gamma < \gamma_{cr}$ is not very dramatic: for $\nu = 2$, $\gamma = 5/3$ we find $P_s/P_0 \propto M_0^4$ instead of $P_s/P_0 \propto M_0^{3.0}$ in Ref. [2]. If, following Ref. [2], we set up an increasing inward entropy profile and simulate cases with $M_0 < 10$, we also observe $P_s/P_0 \propto M_0^{2.5-3.5}$ [in the limit of $M_0 \rightarrow \infty$, Eqs. (17), (19), and (20) apply to the nonuniform entropy profiles as well]. Although the existence of γ_{cr} is not discussed explicitly in Ref. [2], one should be aware that Eqs. (16) and (17) of Ref. [2] become inapplicable for $\gamma > \gamma_{cr}$ and sufficiently large values of M_0 .

In conclusion, we have established how the basic laws of ideal hydrodynamics govern the compression of matter and the increase of the stagnation adiabat in thin fluid shells that are imploded in converging geometries by a fixed external pressure. The derived scaling laws may serve as

valuable guidelines for general analysis of imploding configurations in ICF, and, in particular, for gaining a deeper insight into the scaling laws for a minimum ignition energy [4]. For the latter case, the relationship (20) provides an important link between the in-flight, α_0 , and stagnation, α_s , adiabat parameters. A direct comparison, however, shows no perfect agreement between the formula

$$\alpha_s \propto \alpha_0^{4/5} U_{\max}^{2/3} P_0^{-2/15}, \quad (22)$$

obtained for $\nu = 2$, $\gamma = 5/3$ by substituting $M_0 = U_{\max}(P_0/\rho_0)^{-1/2} = \alpha_0^{-3/10} U_{\max} P_0^{-1/5}$ into our asymptotic law (20), and the scaling

$$\alpha_s \propto \alpha_0^{0.75 \pm 0.01} U_{\max}^{0.44 \pm 0.03} P_0^{-0.21 \pm 0.01}, \quad (23)$$

inferred in Ref. [4] from a large number of fusion capsule simulations. This is not surprising because the fusion capsules have been simulated for a certain intermediate range of Mach numbers, had gas filled central cavities, and included other physical processes (such as heat conduction, alpha-particle heating, etc.) which distort the ideal hydrodynamic profiles used in the present work.

The authors gratefully acknowledge many helpful discussions with A.Kemp. This work was supported by the Bundesministerium für Forschung und Technologie under Contract No. 06MM871.

*On leave from Institute for Theoretical and Experimental Physics, Moscow, Russian Federation.

Electronic address: m.basko@gsi.de

- [1] J. D. Lindl, *Inertial Confinement Fusion* (Springer, New York, 1998).
- [2] A. Kemp, J. Meyer-ter-Vehn, and S. Atzeni, Phys. Rev. Lett. **86**, 3336 (2001).
- [3] J. Meyer-ter-Vehn and C. Schalk, Z. Naturforsch. A **37**, 955 (1982).
- [4] M. C. Herrmann, M. Tabak, and J. D. Lindl, Nucl. Fusion **41**, 99 (2001).
- [5] M. M. Basko, Nucl. Fusion **30**, 2443 (1990).